Software News and Update
A Semiempirical Free Energy Force Field with Charge-Based Desolvation

RUTH HUEY, GARRETT M. MORRIS, ARTHUR J. OLSON, DAVID S. GOODSELL
Department of Molecular Biology, Scripps Research Institute, La Jolla, California 92102

Abstract: The authors describe the development and testing of a semiempirical free energy force field for use in AutoDock4 and similar grid-based docking methods. The force field is based on a comprehensive thermodynamic model that allows incorporation of intramolecular energies into the predicted free energy of binding. It also incorporates a charge-based method for evaluation of desolvation designed to use a typical set of atom types. The method has been calibrated on a set of 188 diverse protein–ligand complexes of known structure and binding energy, and tested on a set of 100 complexes of ligands with retroviral proteases. The force field shows improvement in redocking simulations over the previous AutoDock3 force field.

© 2007 Wiley Periodicals, Inc.   J Comput Chem 28: 1145–1152, 2007

Key words: computational docking; prediction of free energy; force fields; desolvation models; computer-aided drug design; AutoDock4

Introduction

Computational docking currently plays an essential role in drug design and in the study of macromolecular structure and interaction.[1–5] Docking simulations require two basic methods: a search method for exploring the conformational space available to the system and a force field to evaluate the energetics of each conformation. Given the desire to minimize computational effort, there is a trade-off between these two elements. We may choose to use a highly sophisticated force field while searching only a small portion of the conformational space. This is the approach taken by methods such as molecular dynamics and free energy perturbation, which use physically based energy functions combined with full atomic simulation to yield accurate estimates of the energetics of molecular processes.[6] However, these methods are currently too computationally intensive to allow blind docking of a ligand to a protein. Computational docking is typically performed by employing a simpler force field and exploring a wider region of conformational space. This is the approach taken by AutoDock (http://autodock.scripps.edu) and other computational docking methods, which may predict bound conformation with no *a priori* knowledge of the binding site or its location on the macromolecule.[7–9]

Empirical free energy force fields, which define simple functional forms for ligand–protein interactions, and semiempirical free energy force fields, which combine traditional molecular mechanics force fields with empirical weights and/or empirical functional forms, have been used by a wide variety of computa-tional docking methods.[7–9] These force fields provide a fast method to rank potential inhibitor candidates or bound states based on an empirical score. In some cases, this score may be calibrated to yield an estimate of the free energy of binding.

The AutoDock3 force field[10] is an example. It uses a molecular mechanics approach to evaluate enthalpic contributions such as dispersion/repulsion and hydrogen bonding and an empirical approach to evaluate the entropic contribution of changes in solvation and conformational mobility. Empirical weights are applied to each of the components based on calibration against a set of known binding constants. The final semiempirical force field is designed to yield an estimate of the binding constant.

We describe here the development and testing of an improved semiempirical free energy force field for AutoDock4, designed to address several significant limitations of the Auto-Dock3 force field. The new force field, which has been calibrated using a large set of diverse protein–ligand complexes, includes two major advances. The first is the use of an improved thermodynamic model of the binding process, which now allows inclusion of intramolecular terms in the estimated free energy. Second, the force field includes a full desolvation model that includes terms for all atom types, including the favorable energetics of desolvating carbon atoms as well as the unfavorable

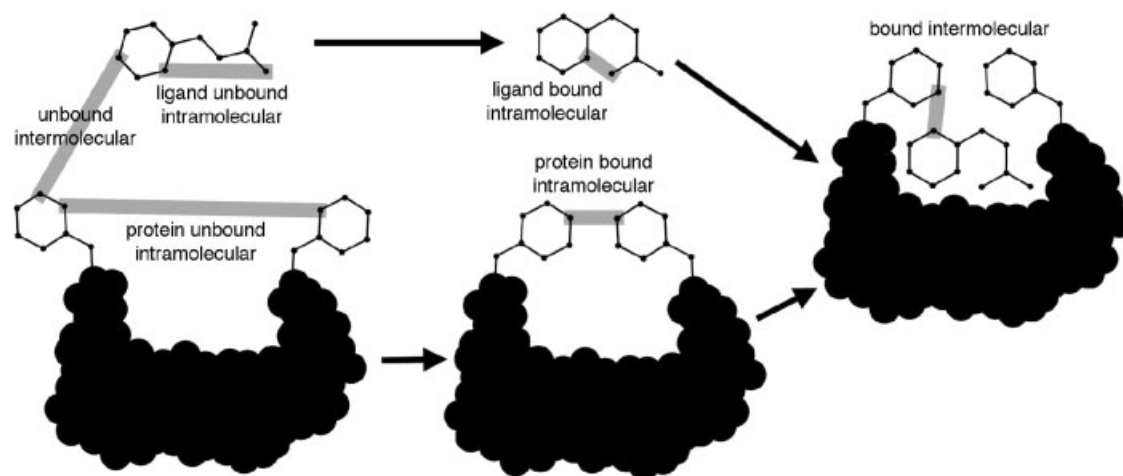*Correspondence to:* D.S. Goodsell; e-mail: goodsell@scripps.edu

Figure 1. The force field evaluates binding in two steps. The ligand and protein start in an unbound conformation. The first step evaluates the intramolecular energetics of the transition from these unbound states to the conformation that the ligand or protein will adopt in the bound complex. The second step evaluates the intermolecular energetics of combining the ligand and protein in their bound conformations.

energetics of desolvating polar and charged atoms. The force field also incorporates an improved model of directionality in hydrogen bonds, now predicting the proper alignment of groups with multiple hydrogen bonds such as DNA bases.[11]

Methods

Overview

The semiempirical free energy force field estimates the energetics of the process of binding of two (or more) molecules in a water environment using pair-wise terms to evaluate the interaction between the two molecules and an empirical method to estimate the contribution of the surrounding water. This differs from a traditional molecular mechanics force field, which also relies on pair-wise atomic terms, but typically uses explicit water molecules to evaluate solvation contributions. The goal of the empirical free energy force field is to capture the complex enthalpic and entropic contributions in a limited number of easily evaluated terms.

The approach taken in AutoDock is shown in Figure 1. The free energy of binding is estimated to be equal to the difference between (1) the energy of the ligand and the protein in a separated unbound state and (2) the energy of the ligand–protein complex. This is broken into two steps for the evaluation: we evaluate the intramolecular energetics of the transition from the unbound state to the bound conformation for each of the molecules separately, and then evaluate the intermolecular energetics of bringing the two molecules together into the bound complex.

The force field includes six pair-wise evaluations (V) and an estimate of the conformational entropy lost upon binding (ΔS_{conf}):

$$\Delta G = (V_{\mathrm{bound}}^{\mathrm{L-L}} - V_{\mathrm{unbound}}^{\mathrm{L-L}}) + (V_{\mathrm{bound}}^{\mathrm{P-P}} - V_{\mathrm{unbound}}^{\mathrm{P-P}})$$
$$+ (V_{\mathrm{bound}}^{\mathrm{P-L}} - V_{\mathrm{unbound}}^{\mathrm{P-L}} + \Delta S_{\mathrm{conf}}) \quad (1)$$

In this equation, L refers to the "ligand" and P refers to the "protein" in a protein–ligand complex; note, however, that the approach is equally valid for any types of molecules in a complex. The first two terms are intramolecular energies for the bound and unbound states of the ligand, and the following two terms are intramolecular energies for the bound and unbound states of the protein. The change in intermolecular energy between the bound and unbound states is in the third parentheses. It is assumed that the two molecules are sufficiently distant from one another in the unbound state that $V_{\mathrm{unbound}}^{\mathrm{P-L}}$ is zero. In the current study, we did not allow motion in the protein, so the bound state of the protein is identical with the protein unbound state, and the difference in their intramolecular energy is zero.

The pair-wise atomic terms include evaluations for dispersion/repulsion, hydrogen bonding, electrostatics, and desolvation:

$$V = W_{vdw} \sum_{i,j} \left(\frac{A_{ij}}{r_{ij}^{12}} - \frac{B_{ij}}{r_{ij}^6} \right) + W_{\mathrm{hbound}} \sum_{i,j} E(t) \left(\frac{C_{ij}}{r_{ij}^{12}} - \frac{D_{ij}}{r_{ij}^{10}} \right)$$
$$+ W_{\mathrm{elec}} \sum_{i,j} \frac{q_i q_j}{\varepsilon(r_{ij}) r_{ij}} + W_{\mathrm{sol}} \sum_{i,j} \left(S_i V_j + S_j V_i \right) e^{(-r_{ij}^2 / 2\sigma^2)} \quad (2)$$

The weighting constants W are the ones that are optimized to calibrate the empirical free energy based on a set of experimentally characterized complexes. The first term is a typical 6/12 potential for dispersion/repulsion interactions. Parameters A and B were taken from the Amber force field.[12] The second term is a directional H-bond term based on a 10/12 potential.[13] The parameters C and D are assigned to give a maximal well depth of 5 kcal/mol at 1.9 Å for O—H and N—H, and a depth of 1 kcal/mol at 2.5 Å for S—H. Directionality of the hydrogen bond interaction $E(t)$ is dependent on the angle t away from ideal bonding geometry and is described fully in previous work.[10,14] Directionality is further enhanced by limiting the number of hydrogen bonds available to each point in the grid to the actual

number of hydrogen bonds that could be formed.[11] Electrostatic interactions are evaluated with a screened Coulomb potential identical with that used in AutoDock3.[15] The final term is a desolvation potential based on the volume (V) of the atoms surrounding a given atom, weighted by a solvation parameter (S) and an exponential term based on the distance.[16] As in the original report, the distance weighting factor σ is set to 3.5 Å.

As in our previous work, this force field is calibrated for a united atom model, which explicitly includes heavy atoms and polar hydrogen atoms. Intramolecular energies are calculated for all pairs of atoms within the ligand (or protein, if it has free torsional degrees of freedom), excluding 1–2, 1–3, and 1–4 interactions.

The term for the loss of torsional entropy upon binding (ΔS_{conf}) is directly proportional to the number of rotatable bonds in the molecule (N_{tors}):

$$\Delta S_{\mathrm{conf}} = W_{\mathrm{conf}} N_{\mathrm{tors}} \tag{3}$$

The number of rotatable bonds include all torsional degrees of freedom, including rotation of polar hydrogen atoms on hydroxyl groups and the like.

Desolvation

The desolvation term is evaluated using the general approach of Wesson and Eisenberg.[17] Two pieces of information are needed (1) an atomic solvation parameter for each atom type, which is an estimate of the energy needed to transfer the atom between a fully hydrated state and a fully buried state [S_i in eq. (2)] and (2) an estimate of the amount of desolvation when the ligand is docked [V_i in eq. (2)]. The amount of desolvation is calculated using a volume-summing method similar to the Stouten et al. method.[16] We have developed a modified approach for the atomic solvation parameters based on the chemical type and the atomic charge of the atom. This approach is designed to use simple set atom types used in AutoDock and other docking methods. Incorporation of the atomic charge into the solvation parameter removes the need to use two discrete charged and uncharged atom types for oxygen and nitrogen. This is particularly useful with hybridized charged groups such as carboxylic acids, which require arbitrary assignment of a formal charge on one oxygen or the other when using previous approaches.

The solvation parameter for a given atom (S, used in the equation above) is calculated as:

$$S_i = (\mathrm{ASP}_i + \mathrm{QASP} \times |q_i|) \tag{4}$$

where q_i is the atomic charge and ASP and QASP are the atomic solvation parameters derived here. The ASP is calibrated using six atom types: aliphatic carbons (C), aromatic carbons (A), nitrogen, oxygen, sulfur, and hydrogen. A single QASP is calibrated over the set of charges on all atom types.

The estimation of the extent of desolvation is calibrated to use atomic volumes calculated as a sphere with radius equal to the contact radius (C/A, 2.00; N, 1.75; O, 1.60; S, 2.00). The amount of shielding in a typical protein was evaluated using the

Table 1. Calibration of the Desolvation Model.

Type	ASP (std error)
C	−0.00143 (0.00019)
A	−0.00052 (0.00012)
N	−0.00162 (0.00182)
O	−0.00251 (0.00189)
H	0.00051 (0.00052)
S	−0.00214 (0.00118)

QASP = 0.01097 (0.00263). Note that these values must be multiplied by the empirically determined weighting factor [W_{sol} in eq. (2)] for the estimate of the free energy.

188 proteins in the calibration set (described later). For each atom in the protein, the volume term in the free energy equation was evaluated:

$$\Delta V_i = \sum_{k \neq i} V_k \times e^{(-r_{ik}^2 / 2\sigma^2)} \tag{5}$$

where the sum is performed over all atoms k in the protein, excluding all atoms in the same amino acid residue as i. The maximal value of ΔV for each amino acid type over the entire set of proteins was then determined. These values were used to perform a least-squares fit of the model to a set of experimental vacuum-to-water transfer energies,[18] to determine values for the atomic solvation parameters ASP and QASP. The program *R* (http://www.r-project.org) was used to perform the fit. Several formulations were tested. The best results were obtained using two carbon types, a nonaromatic (C) and an aromatic (A) type (Table1), where the aromatic type is limited to carbon atoms within aromatic ring structures. The maximum error was 1.88 kcal/mol in that case. Using a single carbon type, the maximum error increased to 3.00 kcal/mol, and use of a single type for all atoms, along with the charge, gave a maximum error of 4.12 kcal/mol.

We used a simple approximation for incorporation of additional atom types in the desolvation model. The ASP is assigned to the average of the values from the six atom types used in the calibration and the same QASP is applied.

Unbound States

This method relies on assignment of an unbound state for the ligand and protein. In this work, we tested three approaches to the unbound state, as shown in Figure 2. These states are simple approximations to the ensemble of unbound conformations, making a few extreme assumptions about which conformations dominate the energetics of the ensemble.

The first approach (the "extended" state) is a fully extended conformation, which models a fully solvated conformation with few internal contacts. A short optimization was performed on the ligand in isolation using a uniform potential inversely proportional to the distance between each pair of atoms. This pushes all atoms as far away from one another as possible.
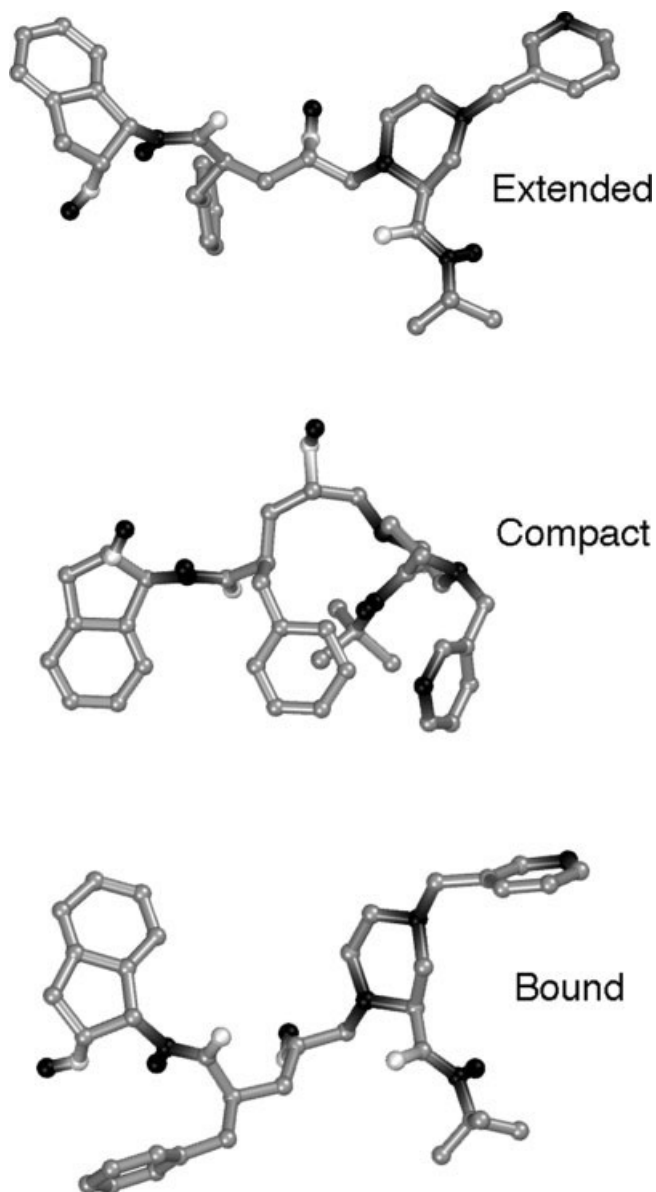
Figure 2. Comparison of the extended, compact, and bound conformations of the HIV protease inhibitor indinavir, taken from PDB entry 1hsg. Note that the extended and bound states are quite similar, and that the hydrophobic groups have formed a cluster in the compact state.

The second approach (the "compact" state) is a minimized conformation that has substantial internal contacts, modeling a folded state for the unbound ligand. We wished to include the new solvation model in the determination of this unbound state, so we used AutoDock4 with values of the energetic parameters taken from the calibration using the extended state. A short Lamarckian genetic algorithm conformational search was performed, using an empty affinity grid. As expected, these conformations tend to bury hydrophobic portions inside and form internal hydrogen bond interactions.

The final approach (the "bound" state) uses the assumption used in AutoDock3 and many other docking methods. In this, it is assumed that the conformation of the unbound state is identical to the conformation of the bound state.

Coordinate Sets

The force field was calibrated and tested using a large collection of protein complexes for which experimental information on binding strength is available. These complexes were taken from two sources.

The force field was calibrated on a set of 188 complexes. Binding data were obtained from the Ligand–Protein Database (http://lpdb.scripps.edu), and coordinates were obtained from the Protein Data Bank (http://www.pdb.org). These complexes were checked and corrected if necessary for the proper biological unit, and files were regularized to remove alternate locations and to have consistent naming of atoms. Hydrogen atoms were then added automatically using Babel,[19] atomic charges were added using the Gasteiger PEOE method,[20] and then nonpolar hydrogen atoms were merged. The Gasteiger method was chosen for its fast and easy operation and ready availability as part of Babel. Formal charges were assigned to metal ions. Charges on terminal phosphate groups were assigned improperly, with a total charge of -0.5, so the remaining -0.5 charge was split manually between the four surrounding oxygen atoms. Babel also treated a sulfonamide group in several ligands as neutral; a single negative charge, as reported in the original structure reports, was split manually between the oxygen and nitrogen atoms in these groups. Ligands were processed in ADT (the graphical interface to AutoDock, http://autodock.scripps.edu/resources/adt) to assign atom types and torsion degrees of freedom. Finally, a short optimization of the ligand was performed using the local search capability of AutoDock3, to relax any unacceptable contacts in the crystallographic conformation.

Binding data for a test set of 100 retroviral protease complexes was obtained from the PDBBind database (http://www.pdbbind.org), and coordinates were obtained from the Protein Data Bank. They were processed similarly to the calibration set.

Redocking

Redocking experiments were performed with AutoDock4 and the new empirical free energy force field. For each complex, 50 docking experiments were performed using the Lamarckian genetic algorithm conformational search with the default parameters from AutoDock3. A maximum of 25 million energy evaluations was applied for each experiment. The results were clustered using a tolerance of 2.0 Å. For comparison, docking experiments with the same parameters were performed with AutoDock3.

Results and Discussion

Performance

The force field was calibrated on a set of 188 complexes tabulated in the Ligand–Protein Database. Calibration with the three
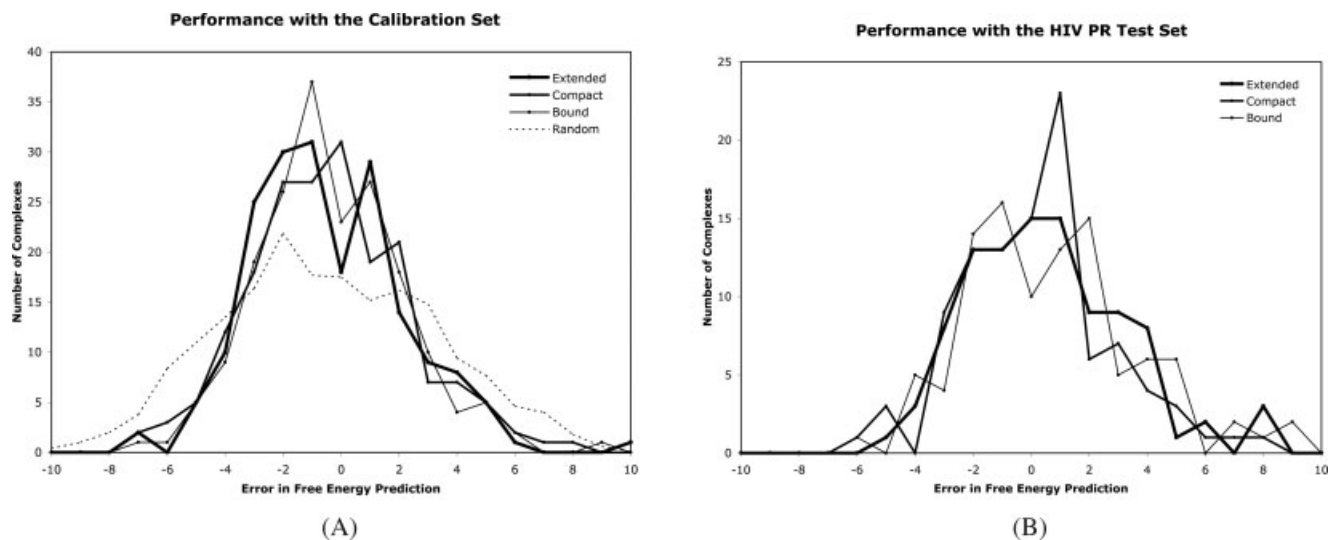
Figure 3. Performance of the new force field. These graphs are histograms showing the number of complexes with a given error in the predicted free energy of binding. Values of zero correspond to complexes that are perfectly predicted, positive values are cases where the predicted energy is too favorable (too negative). The random curve was generated by using a random number between 0 and 1 for values of the h-bond, dispersion/repulsion, electrostatic, and desolvation energies for complexes in the calibration set, and then deriving parameters based on these randomized energies. (A) Results for the calibration set. (B) Results for the HIV protease test set.

different unbound states gave similar results, as shown in Figure 3. Table 2 shows standard errors for the three unbound states for several sets. The first line is standard error over the entire set of 188 complexes used in the calibration. The second line is the standard error calculated for the set of 155 complexes that do not have close ligand–metal contacts, using parameters calibrated against the whole set. The performance is significantly better on this smaller set of proteins. The third line is the standard error when evaluating binding energies for a naive set of 100 HIV protease complexes, not used in the calibration. The final four lines are results from a cross-validation study, where 1/4 of the complexes were removed from the calibration set, and then evaluated with the parameters calibrated with the remaining 3/4 of the set.

Table 3 shows parameters for the three calibrations, including standard errors and t values for the parameters. The compact state is clearly the worst of the three. The extended and bound

states have similar performance, with the bound state showing slightly better statistics in the calibration and the cross-validation, but poorer performance with the HIV test set. Based on these results, we have chosen the extended conformation as the default unbound state in AutoDock4. However, it is possible within AutoDock4 to use any of the models for the unbound state, with the appropriate values for the force field parameters, if there is specific information for a given application about the nature of the unbound state.

The new force field requires slightly more computation time for the energy evaluation than the previous AutoDock3 force field. It requires precalculation of the energy of the unbound state, which is not performed in AutoDock3. During the docking simulation, it requires one additional operation to look-up the charge-dependent desolvation component from a precalculated AutoGrid map.

Magnitude of Terms

The total predicted free energy is surprisingly well distributed between the four pair-wise terms, as shown in Table 4. The dispersion/repulsion term provides an average of about -0.3 to -0.5 kcal/mol per nonhydrogen ligand atom. Hydrogen bonding provides approximately -0.6 kcal/mol for single hydrogen bonds and twice that with oxygen atoms that accept two hydrogen bonds. Electrostatic energies range widely, but give an overall average that is favorable by a few tenths of a kcal/mol. However, in the best cases of interactions with metal ions, electrostatics can provide significant stabilization of several kcal/mol. Desolvation of hydrophobic groups provides a favorable interaction of -0.13 kcal/mol in the best cases and the worst case of

Table 2. Calibration Results.

Coordinate set	Extended	Compact	Bound	AutoDock3
Std error (188 complexes)	2.62	2.72	2.52	2.63
Std error (155 complexes)	2.35	2.51	2.25	2.33
Std error (HIV test set)	2.80	2.52	2.99	3.48
Std error (cross validation)	2.41	2.57	2.36	
	2.44	2.47	2.36	
	2.83	2.92	2.73	
	3.24	3.38	3.07	

Values for standard errors are in kcal/mol.

Table 3. Parameters for the Force Field.

Parameter	Extended	Compact	Bound
1. h-bond	0.097 (0.020) 4.9	0.053 (0.021) 2.5	0.121 (0.022) 5.4
2. desolvation	0.116 (0.026) 4.5	0.060 (0.025) 2.4	0.132 (0.026) 5.0
3. vdw	0.156 (0.009) 17.1	0.164 (0.010) 15.7	0.166 (0.009) 18.0
4. estat	0.147 (0.019) 7.5	0.127 (0.021) 6.1	0.141 (0.019) 7.5
5. tors entropy	0.274 (0.040) 6.9	0.227 (0.040) 5.7	0.298 (0.039) 7.7

Values are given for weight (std error) *t* value.

desolvation of polar oxygen is unfavorable at about +0.6 kcal/mol. Since the desolvation potential is based largely on the atomic charge, note that there are also cases where burial of carbon is unfavorable, as with the carbon atoms in the middle of guanidinium or carboxyl groups.

For the polar atoms, the desolvation term has the desired effect of counterbalancing the hydrogen bonding energy. Hydrogen bonds in complexes do not add substantially to the binding free energy, since they simply replace hydrogen bonds that are formed with water in the free state. When polar groups are buried in proteins without forming hydrogen bonds, however, this can have an unfavorable effect on binding. The combination of the favorable hydrogen bond potential with the unfavorable desolvation potential models this effect in the force field. Polar atoms that form hydrogen bonds in the complex will have a slightly favorable contribution to the energy, but polar atoms that do not form hydrogen bonds will only have the unfavorable desolvation component.

Intramolecular Energies

One of the major advances incorporated into this force field is the inclusion of intramolecular energies in the estimated free energy of binding. Often, these are not included in empirical free energy force fields, causing a persistent problem: the function used for scoring during docking is not the same function used to predict the free energy of binding. In many cases, this is solved by using a simple yes-or-no scoring for intramolecular energies; conformations with unacceptable clashes are simply discarded, so the intramolecular energy is not included explicitly in the scoring function. In AutoDock3, a pair-wise intramolecular energy is used in scoring and optimization, but omitted when

the free energy is predicted for the best conformations. This has an undesirable effect: occasionally a complex will rank high in docking score, but will have a poor free energy, or the converse.

The current method incorporates the intramolecular energy through the use of an unbound structure, so that the difference in energy between the bound and unbound forms is included in the predicted free energy. In most cases, this is close to zero.

Desolvation

The desolvation method used here builds upon two approaches. The basic approach is taken from work from Wesson and Eisenberg.[17] They postulate that the desolvation energy is proportional to the change in the surface area that is available to water. The amount of shielding upon binding is determined by comparing the solvent accessible surface area of the unbound and bound forms. Each type of atom makes a different contribution to this energy, depending on how polar or hydrophobic it is. They classified atoms into a few simple atom types, each with its own atomic solvation parameter. Typically, this set includes two carbon types, one type for polar O or N, and separate types for charged N and charged O. In cases where the charge is delocalized over several atoms (carboxylates, guanidinium), the charge is placed on the most solvent-exposed atom. Stouten et al.[16] modify this basic approach, casting it into a form that is amenable to a pair-wise volume-summing method to evaluate the amount of shielding.

The approach used here was chosen to accommodate the needs of the grid-based evaluation used in AutoDock and many other methods. The number of atom types must be kept to a minimum, since each new atom type requires a new map of interaction potentials. For this reason, we calibrated the method

Table 4. Magnitude of Terms.

Type	Disp/rep	H-bond	Electrostatics	Desolvation
C	+0.14 (−0.43) −0.82	n/a	+1.00 (−0.04) −0.85	+0.48 (+0.01) −0.13
A	+0.00 (−0.41) −0.80	n/a	+0.31 (−0.02) −0.83	+0.75 (+0.02) −0.05
N	−0.02 (−0.34) −0.56	0.00 (−0.03) −0.59	+0.54 (−0.25) −3.67	+0.56 (+0.11) −0.08
O	+0.17 (−0.32) −0.68	0.00 (−0.23) −1.24	+1.52 (−0.09) −7.07	+0.60 (+0.10) −0.06
S	−0.15 (−0.54) −0.93	0.00 (−0.01) −0.11	+0.05 (−0.01) −0.10	+0.00 (−0.08) −0.15
H	+0.09 (−0.05) −0.11	0.00 (−0.32) −0.63	+1.14 (−0.21) −1.15	+0.35 (+0.18) +0.00

Minimum (average) maximum values in kcal/mol evaluated over all ligand atoms in the set of 188 complexes from the calibration set. A includes aromatic carbons, and C includes all other carbon atoms. N, O, and S include only those nitrogen, oxygen, and sulfur atoms that accept hydrogen bonds. H includes polar hydrogen atoms.

Table 5. Parameters Calibrated with the Reduced set of 155 Complexes.

Parameter	Weight (std error)	*t* value
1. h-bond	0.172 (0.020)	8.416
2. desolvation	0.065 (0.024)	2.621
3. vdw	0.090 (0.008)	17.184
4. estat	−0.014 (0.034)	−0.424
5. tors entropy	0.336 (0.036)	9.292

using simple volumes calculated from contact radius, instead of more complex atomic volumes used in the Stouten et al. formulation. To account for the differences in polar atoms with a formal charge and those without, we incorporated a term based on the charge, instead of breaking oxygen and nitrogen atoms into two or more types.

Electrostatics

A slightly improved performance may be obtained by calibrating the force field using only the 155 complexes with no close ligand–metal contacts, with a standard error of 2.25 kcal/mol (compared with 2.35 kcal/mol using parameters calibrated from the entire set). The disadvantage, however, is that this formulation leads to a parameterization that does not include an electrostatic term, as shown in Table 5. These results are presented for
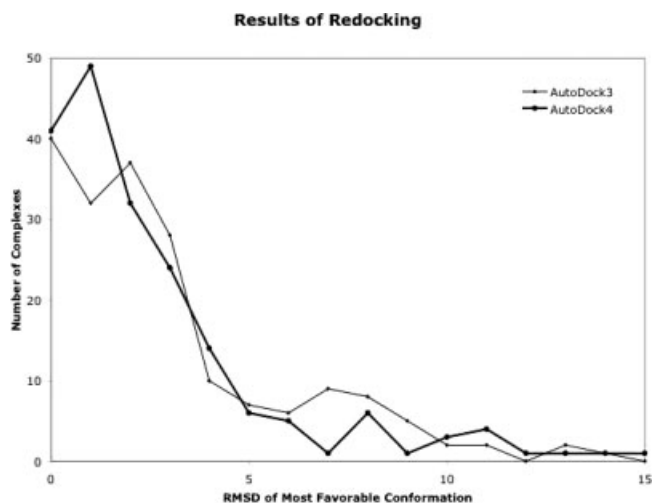

Figure 4. Performance of the new force field in docking experiments, compared with AutoDock3. The graph is a histogram showing the number of complexes within a given RMSD of the crystallographic structure. In each case, the conformation with most favorable estimated energy is used as the predicted conformation.

the extended state of the unbound ligand; similar results were obtained using the other two approximates for the unbound state. Note that the statistics for the electrostatic term are poor; in
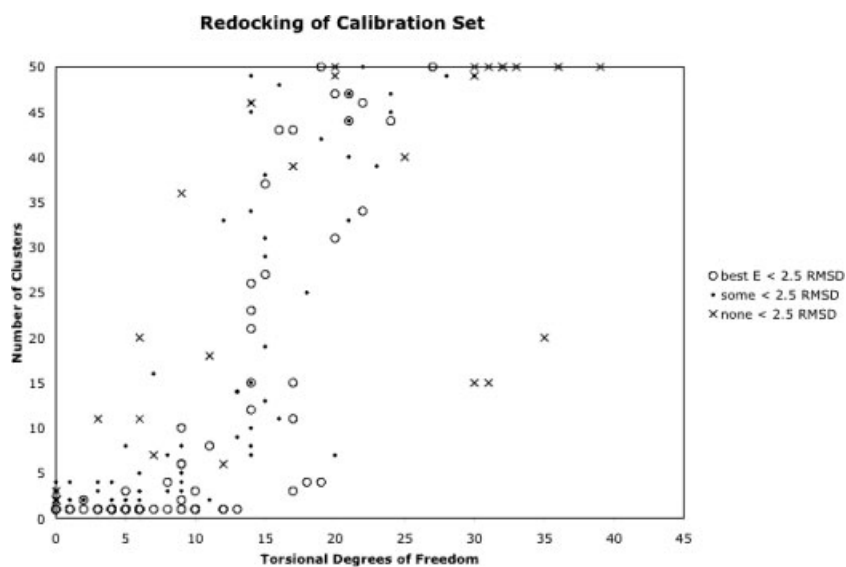

Figure 5. Performance of the new force field in redocking experiments. Each point in the graph represents one protein–ligand complex in the calibration set. Open circles are cases where the conformation of best predicted energy is within 2.5 Å of the crystallographic conformation. Dots are cases where AutoDock finds a conformation within 2.5 Å of the crystallographic conformation, but it is not the best energy. Complexes that were not successfully redocked are shown with an X. In each case, 50 docking simulations were performed and results that were within 2.0 Å of each other were clustered. The vertical axis shows the number of clusters found for each complex (ideally, if AutoDock was able to find the global minimum structure, we would see one cluster). The horizontal axis shows the number of torsional degrees of freedom in the ligand. Note that AutoDock fails with ligands with greater than 15–20 rotatable bonds.

fact, the model is not significantly affected if the electrostatic term is removed. Instead, the contribution of electrostatics appears to be included in the hydrogen-bonding term, which increases by a factor of two over the full force field described above. This is caused by the fact that there are very few electrostatic interactions within this dataset that do not involve hydrogen bonds. In the reduced set, there are not enough examples to separate the effect of hydrogen bonding from ionic interactions. In the full force field calibration, the metal ion contacts controlled the weighting of the electrostatic term.

Conformational Entropy

We tested two models for evaluation of conformational entropy, both based on a simple sum of the torsional degrees of freedom. The first includes all degrees of freedom and the second excludes terminal rotors that only move hydrogen atoms, such as rotation of hydroxyl groups or amines. Use of all torsional degrees of freedom gave slightly better results: standard error of 2.62 kcal/mol compared with standard error of 2.70 when hydrogen rotors are excluded.

Redocking

We tested the new semiempirical free energy force field in a redocking experiment with the calibration set of 188 protein–ligand complexes. The new force field when used in AutoDock4 performs better than similar redocking experiments using AutoDock3, as shown in Figure 4. In 85 cases, AutoDock4 with the new force field found a conformation within 2.5 Å of the known conformation, and scored this conformation with the best estimated free energy. In 75 cases, the correct conformation was found, but an alternative conformation was scored with better energy. However, in 67 of these cases, the proper conformation and the noncrystallographic conformation were scored within 1 kcal/mol of each other, which is not a significant difference given the precision of the force field. The remaining 28 complexes were not predicted correctly by AutoDock 4, most cases due to the fact that they were very large ligands with greater than 15 degrees of torsional freedom (see Fig. 5).

Conclusions

The performance of the new force field is similar to the existing AutoDock3 force field, which has shown proven effectiveness in hundreds of laboratories.[21] The advantage of the new force field is that it is based on a comprehensive thermodynamic model, which is extensible for use in protein–protein docking and for incorporation of protein flexibility. The new force field has the strong advantage of incorporating the intramolecular energy into

the calculation, and has a conceptually satisfying formulation for the desolvation that includes terms for all atoms and does not require any assumptions for placement of charges. The force field will be made available with the release of AutoDock version 4.

Acknowledgment

References

1. Schneider, G.; Bohm, H. J. Drug Discovery Today 2002, 7, 64.
2. Alvarez, J. C. Curr Opin Chem Biol 2004, 8, 365.
3. Oprea, T. I.; Matter, H. Curr Opin Chem Biol 2004, 8, 349.
4. Kitchen, D. B.; Decornez, H.; Furr, J. R.; Bajorath, J. Nat Rev Drug Discov 2004, 3, 935.
5. Mohan, V.; Gibbs, A. C.; Cummings, M. D.; Jaeger, E. P.; DesJarlais, R. L. Curr Pharm Des 2005, 11, 323.
6. Wang, W.; Donini, O.; Reyes, C. M.; Kollman, P. A. Annu Rev Biophys Biomol Struct 2001, 30, 211.
7. Halperin, I.; Ma, B.; Wolfson, H.; Nussinov, R. Proteins: Struct Funct Genet 2002, 47, 409.
8. Taylor, R. D.; Jewsbury, P. J.; Essex, J. W. J Comput Aided Mol Des 2002, 16, 151.
9. Brooijmans, N.; Kuntz, I. D. Annu Rev Biophys Biomol Struct 2003, 32, 335.
10. Morris, G. M.; Goodsell, D. S.; Halliday, R. S.; Huey, R.; Hart, W. E.; Belew, R. K.; Olson, A. J. J Comput Chem 1998, 19, 1639.
11. Huey, R.; Goodsell, D. S.; Morris, G. M.; Olson, A. J. Lett Drug Des Discov 2004, 1, 178.
12. Weiner, S. J.; Kollman, P. A.; Case, D. A.; Singh, U. C.; Ghio, C.; Alagona, G.; Profeta, S.; Weiner, P. J Am Chem Soc 1984, 106, 765.
13. Goodford, P. J. J Med Chem 1985, 28, 849.
14. Boobbyer, D. N. A.; Goodford, P. J.; McWhinnie, P. M.; Wade, R. C. J Med Chem 1989, 32, 1083.
15. Mehler, E. L.; Solmajer, T. Protein Eng 1991, 4, 903.
16. Stouten, P. F. W.; Frommel, C.; Nakamura, H.; Sander, C. Mol Simul 1993, 10, 97.
17. Wesson, L.; Eisenberg, D. Protein Sci 1992, 1, 227.
18. Sharp, K. A.; Nicholls, A.; Friedman, R.; Honig, B. Biochemistry 1991, 30, 9686.
19. Tetko, I. V.; Gasteiger, J.; Todeschini, R.; Mauri, A.; Livingstone, D. J.; Ertl, P.; Palyulin, V. A.; Radchenko, E. V.; Zefirov, N. S.; Makarenko, A. S.; Tanchuk, V. Y.; Prokopenko, V. V. J Comput Aided Mol Des 2005, 19, 453.
20. Gasteiger, J.; Marsili, M. Tetrahedron 1980, 36, 3219.
21. Sousa, S. F.; Fernandes, P. A.; Ramos, M. J. Proteins 2006, 65, 15.